

# On the characterization of oxygen recombination in sealed lead-acid batteries

H. DIETZ, M. RADWAN, J. GARCHE, H. DÖRING, K. WIESENER

*Dresden University of Technology, Chemistry Department, Mommsenstrasse 13, 8027 Dresden, GDR*

Received 11 July 1989; revised 30 May 1990

For characterizing the oxygen cycle in sealed lead-acid batteries the technological terms “oxygen recombination efficiency” and “oxygen recombination conditions” are introduced and their different meanings explained. Numerical values are calculated or estimated from plots of overpressure against time. Emphasis is placed on investigations of the influence of technological parameters on oxygen recombination conditions.

## Nomenclature

$F$	Faraday constant	$I_{\text{H}_2\text{ev}}$	hydrogen evolution current
$D$	diffusion coefficient	$I_{\text{PbSO}_4\text{red}}$	cathodic formation (recharge) current
$L$	solubility coefficient	$p_{\text{O}_2}$ (st)	steady-state $p_{\text{O}_2}$
$A$	effective surface area on the negative electrode covered with an electrolyte film	$p_{\text{O}_2}$	quasi steady-state $p_{\text{O}_2}$
$\delta$	diffusion layer thickness	$R$	gas constant
$p_{\text{O}_2}$	oxygen partial pressure	$T$	temperature
$p_{\text{H}_2}$	hydrogen partial pressure	$V$	gas space volume
$I_{\text{OC}}$	overcharging current (defined negative)	$\Delta$	$(I_{\text{OC}} - I_{\text{O}_2\text{red}} - I_{\text{H}_2\text{ev}})$
$I_{\text{O}_2\text{red}}$	oxygen reduction current	$\eta$	viscosity
		$d$	electrode distance
		$l$	crack length
		$\rho$	electrolyte density

## 1. Introduction

In contrast with classical lead-acid batteries, sealed types require additional precautions for minimizing gas evolution and for gas recombination. Gas recombination reactions are kinetically hindered but to a different extent [1]. The hydrogen oxidation at the working potential of the positive electrode is strongly limited [2, 3, 4]. Also the direct  $\text{H}_2$ - $\text{O}_2$ -recombination only takes place in the presence of a catalyst. On the other hand, the oxygen reduction at the negative electrode can proceed at a considerably higher rate [2, 5, 6, 7], if one provides for rapid oxygen transport from the positive to the negative electrode. This is because oxygen reduction in  $\text{H}_2\text{SO}_4$  solution is under diffusion control [2, 8–11].

As the diffusion coefficient of oxygen in the gas phase is several times higher than in liquid  $\text{H}_2\text{SO}_4$  solution, in sealed lead-acid batteries the electrolyte is immobilized, i.e. the oxygen is transferred either via voids in adsorptive separator systems or via micro-cracks in a gelled electrolyte. In this paper, we refer to the mechanism of oxygen transport in micro-cracks of gelled electrolytes. As a result of crack formation, the diffusion path length in the liquid diminishes and is assumed to reach the order of magnitude of the diffusion layer thickness.

$$J_{\text{O}_2\text{red}} = zFDLAp_{\text{O}_2}/\delta \quad (1)$$

As can be seen from the modified diffusion formula, Equation 1 [12, 13], further increase of the oxygen reduction rate can be obtained by (i) increasing the oxygen partial pressure  $p_{\text{O}_2}$  and (ii) improving oxygen recombination conditions ( $A/\delta$ ), i.e. increasing  $A/\delta$ , where  $A$  is the effective surface area of the negative electrode directly accessible to oxygen and covered with a thin electrolyte film.

In order to model the gas material balance of sealed cells [12, 13] and to estimate the oxygen recombination conditions at the negative electrode [12–15], measuring the cell overpressure during galvanostatic overcharging and after circuit interruption is a suitable method. The oxygen recombination efficiency during overcharging, defined in this paper as the portion of the total current that represents the oxygen reduction current, can be determined from the same measurements (see §3.1). Previously this was roughly calculated gravimetrically and volumetrically after measuring the mass loss of water [6, 16] or the total quantity of vented gas [7]. However, only the combined technique of determining both total gassing rate and gas composition offers precise calculation [14, 17]. For analysing the gas composition, gas chromatography is an accurate though expensive method [17].

The purpose of this paper, therefore, is to present a simple method of obtaining information on both oxygen recombination conditions and efficiency by analysing plots of overpressure against time recorded

during galvanostatic overcharging of sealed lead-acid batteries. The effect of technological parameters and oxygen partial pressure is also investigated.

## 2. Experimental details

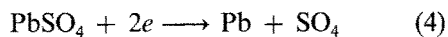
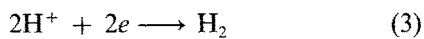
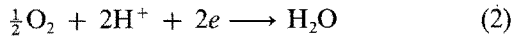
The cell-vessels used in our experiments were made of PVC and comprised one positive electrode arranged between two negative electrodes. The grid material was pure lead, the electrolyte was  $\text{H}_2\text{SO}_4$  ( $\rho = 1.28 \text{ g cm}^{-3}$ ) immobilized by Aerosil R-300. If not described otherwise, dry-charged 3 Ah electrodes of dimensions  $45 \text{ mm} \times 80 \text{ mm} \times 2 \text{ mm}$  were used, the inter electrode distance was 2 mm and the cell, having a gas space of  $24 \text{ cm}^3$ , was filled under evacuation with 60 g  $\text{H}_2\text{SO}_4$  gel containing 6% Aerosil.

The upper edges of the electrodes were always covered with electrolyte. Before the measurements the electrodes were recharged at a current of 300 mA for 1 h. The the gas space of the cell was purged with pure nitrogen. After this procedure the cell was sealed and thermostated at  $23^\circ\text{C}$ . The cell overpressure was measured by means of a pressure sensor type DHW 10030 that transformed the measured values into continuously recorded electric signals. Galvanostatic overcharging was carried out at a current of 300 mA.

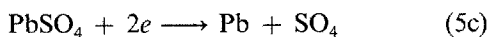
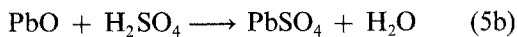
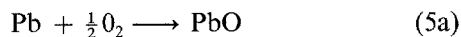
## 3. Results and discussion

### 3.1. Method of evaluation

During overcharging of sealed lead-acid batteries the following three cathodic reactions must be considered:



With respect to the mechanism of the oxygen reduction reaction, it should be noted that either the reaction sequence 5a–5c (corrosion mechanism [3, 18] followed by re-charge) or a mixture of both the mechanisms 5a–c and 3 [19, 20] are possible but unproven.



From the anodic processes, only the oxygen evolution reaction, has to be taken into account. This is because the other partial currents of subsequent  $\text{PbO}_2$  formation, grid corrosion,  $\text{CO}_2$  evolution as well as  $\text{H}_2$  oxidation were found to be negligible at low polarizations [17, 21].

Thus, for galvanostatic overcharging with the overcharging current,  $I_{\text{OC}}$ , Equation 6 follows.

$$|I_{\text{OC}}| = I_{\text{O}_2\text{ev}} = |I_{\text{O}_2\text{red}} + I_{\text{H}_2\text{ev}} + I_{\text{PbSO}_4\text{red}}| \quad (6)$$

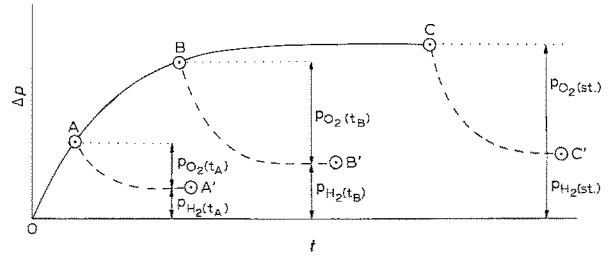


Fig. 1. Idealized course of cell overpressure during galvanostatic overcharging (O–A–B–C) and after circuit interruption (A–A' . . . C–C').

This equation describes the overpressure course during galvanostatic overcharging (Fig. 1).

Whereas oxygen evolution proceeds at the constant rate of  $I_{\text{OC}}$ , i.e. proportional to time, the oxygen reduction rate at the negative electrode increases with increasing  $p_{\text{O}_2}$ . In the ideal case, when the oxygen reduction rate becomes equal to the oxygen evolution rate, a steady-state overpressure appears (Fig. 1, point C).

The pressure drop observed after circuit interruption (Fig. 1; A–A'; B–B' . . .) is due to currentless oxygen recombination and therefore corresponds to  $p_{\text{O}_2}$  at the end of overcharging (Fig. 1, A, B . . .). The remaining overpressure, caused by  $\text{H}_2$  evolution during overcharging, corresponds to  $p_{\text{H}_2}$ . Hence, the steady-state pressure of oxygen  $p_{\text{O}_2}(\text{st})$  can be obtained from the oxygen decay at open circuit (Fig. 1, C–C') after reaching the steady state (Fig. 1,  $t = C$ ). Under steady-state conditions  $I_{\text{O}_2\text{red}}$  equals  $I_{\text{OC}}$  and consequently it becomes constant. With Equation 1, it follows, that  $p_{\text{O}_2}(\text{st})$  is a specific criterion for the oxygen recombination conditions  $A/\delta$  (Equation 7) than can be also calculated from the rate of  $p_{\text{O}_2}$  decay at open circuit [12–15, 22].

$$p_{\text{O}_2}(\text{st}) \sim (A/\delta)^{-1} \quad (7)$$

As an oxygen recombination efficiency of 100% within a finite period of time will not be attained, in sealed lead-acid cells, only a quasi steady-state pressure of oxygen ( $p_{\text{O}_2}^*$ ) can be reached. Therefore, for the following investigations, the oxygen recombination conditions were only estimated using the approximation  $p_{\text{O}_2}(\text{st}) \approx p_{\text{O}_2}^*$ .

In practice (short periods of overcharging) even the quasi steady-state cannot be realized. Therefore,  $I_{\text{O}_2\text{red}}$  or its fraction of  $I_{\text{OC}}$ , which can be understood as oxygen recombination efficiency when using fully charged positive electrodes, depends on  $A/\delta$ ,  $p_{\text{O}_2}$  and the conditions of the other competing reactions at the negative electrode.

The instantaneous values of  $I_{\text{O}_2\text{red}}$  or  $I_{\text{Hev}}$  as well as their percentage of  $I_{\text{OC}}$  can be evaluated as an average current of any overcharge period AB from the difference increase in  $p_{\text{O}_2}$  or  $p_{\text{H}_2}$  according to Equations 2, 3, 8, 9 and Fig. 1. Thus,  $I_{\text{O}_2\text{red}}$  is obtained from  $I_{\text{OC}}$  by subtracting the current portion that corresponds to the oxygen amount, which cannot be recombined (Equation 8).

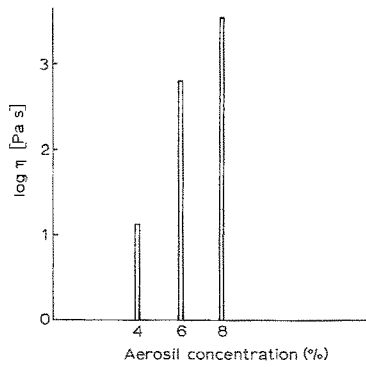


Fig. 2. Results from viscosity measurements on H<sub>2</sub>SO<sub>4</sub> gels showing dependence on gel former concentration, (mixing time: 1 min).

$$I_{O_2,red} = I_{OC} - \left( \frac{P_{O_2}(t_A) - P_{O_2}(t_B)}{t_B - t_A} \right) \left( \frac{4F}{RT/V} \right) \quad (8)$$

$$I_{H_2,ev} = \left( \frac{P_{H_2}(t_A) - P_{H_2}(t_B)}{t_B - t_A} \right) \left( \frac{2F}{RT/V} \right) \quad (9)$$

3.2. Influence of technological parameters on oxygen recombination conditions

The formation of thixotropic H<sub>2</sub>SO<sub>4</sub> gels is known to begin at gel former concentrations of about 3–5% [23, 24]. Simultaneously, microcracks are formed within the electrolyte, thus providing pathways for gas transport. The viscosity of the gel electrolyte seems to be directly related to, and a measure of, the number of microcracks formed.

To estimate the extent of microcrack formation, viscosity measurements have therefore been carried out (Fig. 2). Our measurements confirmed results of similar experiments performed by Orkina *et al.* [25] and showed that increasing the gel former concentration leads to an increase in viscosity and microcrack formation. As a main consequence the effective surface area, *A*, is assumed to increase (Fig. 7a–b<sub>1</sub>), thus explaining the improvement in oxygen recombination conditions, i.e. the decrease in *p*<sub>O<sub>2</sub></sub> (Fig. 3).

Only running cracks are utilizable for oxygen transport from the positive to the negative electrode. It can therefore be supposed that decreasing the electrode distance (from *d*<sub>1</sub> to *d*<sub>2</sub>) enables additional microcracks (of length *l*<sub>1</sub> between *d*<sub>1</sub> and *d*<sub>2</sub>) to contribute to oxygen transfer (Fig. 7c–d), thus increasing *A* (Fig.

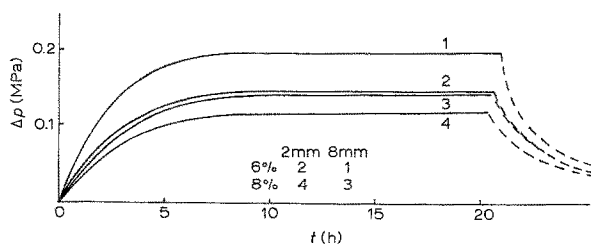


Fig. 3. Influences of electrode distances and gel former concentration on cell pressure characteristics during galvanostatic overcharging (*I*<sub>OC</sub> = 300 mA) and after circuit interruption, (90 g of H<sub>2</sub>SO<sub>4</sub> gel, electrode dimensions: 45 mm × 45 mm × 2 mm).

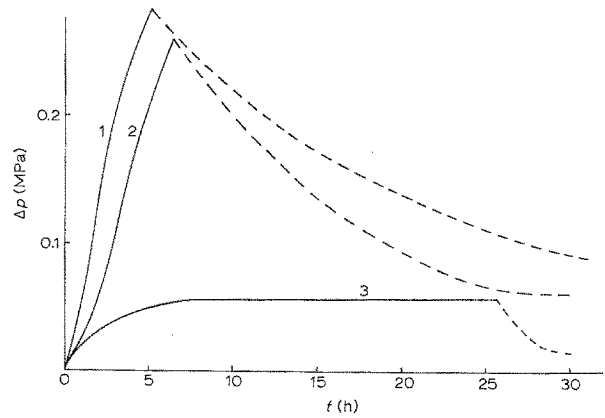


Fig. 4. Effects of conditions of application of electrodes (pretreatment) on cell pressure characteristics during galvanostatic overcharging (*I*<sub>OC</sub> = 300 mA) and after circuit interruption. (1) electrolyte-wet electrode, under evacuation, (2) dry electrodes, without evacuation, (3) dry electrodes, under evacuation.

7b<sub>1</sub>, 7b<sub>2</sub>). This is confirmed by Fig. 3, which indicates improvement in oxygen recombination conditions.

Figure 4 demonstrates the effects of different methods of gel preparation and cell filling. Due to capillary forces, the electrodes placed in the cell in a dry state, especially the additionally evacuated ones, are able to soak in H<sub>2</sub>SO<sub>4</sub> from the gel electrolyte, in contrast to acid-immersed electrodes. This process leads to the same consequences as the increase in gel former concentration, i.e., additional crack formation and increase in reaction surface area (Fig. 7a–b<sub>2</sub>). Thus, the oxygen recombination conditions are improved considerably (Fig. 4).

The oxygen recombination conditions can also be improved by minimizing the amount of electrolyte (Fig. 5) with the practical limit for satisfying Ah-capacity output being 40 g. This can be explained as follows. Since the amount of acid adsorbed by the active masses remains constant and the gel former does not penetrate into the active masses [26] the effective concentration of the gel former in the gelled bulk electrolyte increases, thus producing additional running cracks (Fig. 7d–e).

Figure 6 illustrates the influence of the state-of-charge of the negative electrode. Partial discharge diminishes the area of free lead sites and consequently the effective surface area, *A*. As a result, the oxygen recombination conditions become worse.

3.3. Influence of *p*<sub>O<sub>2</sub></sub> on the oxygen recombination efficiency

The cathodic current fractions of *I*<sub>OC</sub> calculated from

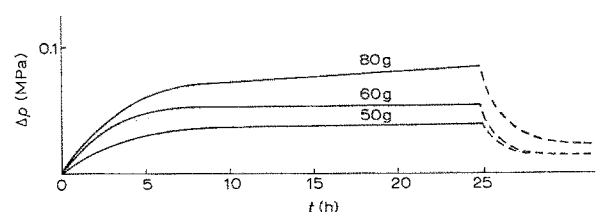


Fig. 5. Influence of amount of electrolyte on cell pressure characteristic during galvanostatic overcharging (*I*<sub>OC</sub> = 300 mA) and after circuit interruption.

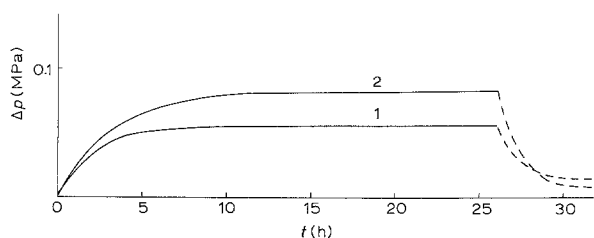


Fig. 6. Influence of state-of-charge of negative electrodes on cell pressure characteristic during galvanostatic overcharging ( $I_{OC} = 300$  mA) and after circuit interruption. (1) fully charged, (2) 2/3 charged (67%  $C_{20}$ ).

Equations 8 and 9 are presented in Fig. 8. The following can be seen:

1. The oxygen recombination efficiency increases with increasing  $p_{O_2}$ , thus suppressing hydrogen evolution.
2. There is a difference,  $\Delta$ , between  $I_{OC}$  and the sum of  $I_{O_2,red}$  and  $I_{H_2,ev}$ . This difference mainly corresponds to an additional cathodic current  $I_{PbSO_4,red}$  which increases the state-of-charge of the negative electrode, as we have confirmed analytically. Partially, following the gas-balance approach of Maja *et al.* [13],  $\Delta$  may also be caused by hydrogen oxidation at the positive electrode. Assuming this, the hydrogen oxidation current is overcompensated for by hydrogen evolution, the rate of which should be somewhat higher than expected according to Equation 9.
3. If  $\Delta$  is interpreted as  $I_{PbSO_4,red}$  it is also the decrease in the  $PbSO_4$  reserve of the negative electrode that prevents the hydrogen evolution from becoming too intensive. This is particularly seen at low  $p_{O_2}$ , i.e. at the beginning of overcharging.

#### 4. Conclusion

Under overcharging conditions, i.e. provided that the oxygen evolution is the only anodic process, the oxygen recombination efficiency can be defined as a fraction  $I_{O_2,red}$  of  $I_{OC}$ . It is a measure of the instantaneous value of the oxygen reduction current

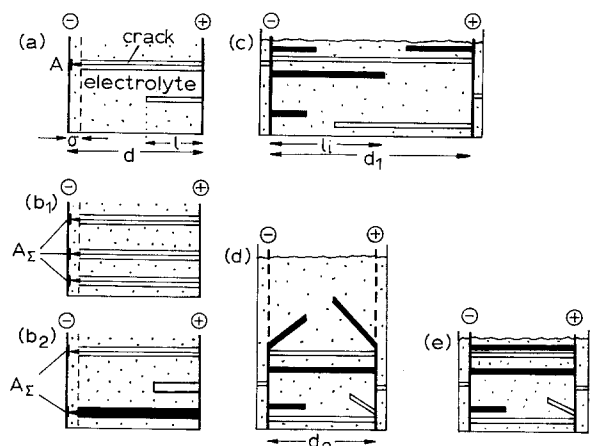


Fig. 7. Model of principal influences of technological parameters on oxygen recombination conditions. (a-b<sub>1</sub>) increase in gel former concentration, (a-b<sub>2</sub>) evacuation, (c-d) decrease in interelectrode distance, (d-e) decrease in amount of electrolyte. (□) crack formation caused by electrolyte gelling, (■) crack formation caused by  $H_2SO_4$  soaking into the mass pores of the electrodes.

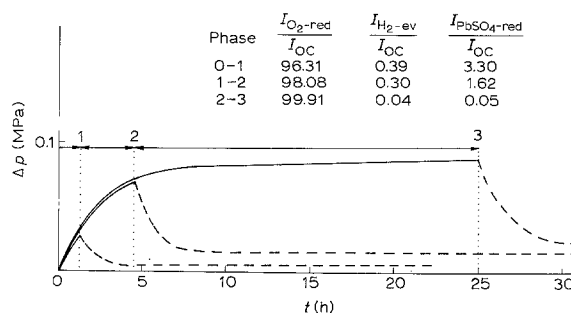


Fig. 8. Alterations in the fractions of the cathodic partial currents at the negative electrode during galvanostatic overcharging.  $I_{OC} = 300$  mA, 80 g of  $H_2SO_4$  gel. Note. Mean values of all partial currents calculated according to Equations 8 and 9. Values of  $p_{O_2}$  and  $p_{H_2}$  determined by means of pressure decay curves.

that depends on the oxygen recombination conditions  $A/\delta$  and  $p_{O_2}$  as well as on the conditions of the other competing reactions, i.e.  $H_2$  evolution and  $PbSO_4$  reduction. It can be obtained from  $I_{OC}$  and the portion of the amount of oxygen which cannot be recombined via analysis of overpressure decay during overcharging.

Values for oxygen recombination conditions, however, can be computed only from data on the steady-state pressure i.e. at an oxygen recombination efficiency of 100%. The quasi steady-state  $p_{O_2}$ , which is reached only after a long period of galvanostatic overcharging, has proved to be a suitable criterion for estimating these conditions.

The oxygen recombination conditions will be improved by increasing the gel former concentration, diminishing the amount of electrolyte and the distance between the electrodes, and also by evacuation. These measures, as well as the increase in  $p_{O_2}$ , lead to suppression of hydrogen evolution.

#### References

- [1] C. S. C. Bose and N. A. Hampson, *J. Power Sources*, **19** (1987) 261.
- [2] B. K. Mahato, E. Y. Weissmann and E. C. Laird, *J. Electrochem. Soc.* **121** (1974) 13.
- [3] P. Ruetschi and R. T. Angstadt, *ibid.* **105** (1958) 555.
- [4] I. A. Aguf and N. K. Grigalyuk, *Sov. Electrochem.* **19** (1983) 965.
- [5] B. K. Mahato and E. C. Laird, in 'Power Sources 5', (edited by D. H. Collins), Academic Press, London (1975) p. 23.
- [6] B. Culpin, K. Peters and N. R. Young, in 'Power Sources 9', (edited by J. Thompson), Academic Press, London (1983) p. 129.
- [7] A. I. Harrison and B. A. Wittey, in 'Power Sources 10', (edited by L. J. Pearce), The Paul Press London (1985) p. 447.
- [8] A. N. Fleming, I. A. Harrison and J. Thompson, in 'Power Sources 5', (edited by D. H. Collins), Academic Press, London (1975) p. 1.
- [9] J. Thompson and S. Warrel, in 'Power Sources 9' (edited by J. Thompson), Academic Press, London (1983), p. 97.
- [10] R. D. Armstrong and K. L. Bladen, *J. Appl. Electrochem.* **7** (1977) 345.
- [11] E. A. Khomskaya, N. F. Gorbacheva and N. B. Tolochkov, *Sov. Electrochem.* **16** (1980) 48.
- [12] J. Garche, D. Ohms, H. Dietz, N. D. Hung, K. Wiesener and J. Mrha, *Electrochim. Acta* **34** (1989) 1603.
- [13] M. Maja and N. Penazzi, *J. Power Sources* **25** (1989) 99.
- [14] *Idem, ibid.* **25** (1989) 229.
- [15] J. Mrha, U. Vogel, S. Kreuels und W. Vielstich, *ibid.* **27** (1989) 201.

- [16] J. Szymborski and B. Burrows, in 'Power Sources 9' (edited by J. Thompson), Academic Press, London (1983) p. 113.
- [17] J. S. Symanski, B. K. Mahato and K. R. Bullock, *J. Electrochem. Soc.* **135** (1988) 548.
- [18] K. Peters and N. R. Young, in 'Advances in Lead-Acid Batteries' (edited by K. R. Bullock and D. Pavlov), Pennington (1984) p. 481.
- [19] K. R. Bullock, *ibid* (1984) p. 1.
- [20] J. Mrha, K. Micka, J. Jindra, and M. Musilova, *J. Power Sources* **27** (1989) 91.
- [21] H. Dietz, S. Voß, H. Döring, J. Garche and K. Wiesener, *J. Power Sources*, in press.
- [22] A. Arlanch, G. Clerici, M. Maja and N. Penazzi, in 'Power Sources 10', (edited by L. J. Pearce), The Paul Press, London (1985) p. 295.
- [23] K. Eberts, in 'Power Sources 2', (edited by D. H. Collins), Pergamon Press, London (1968) p. 69.
- [24] O. Jache, K. S. Pat. 3 172 782 (1965).
- [25] T. N. Orkina, I. A. Aguf, M. A. Dasoyau, *Sb. Rab. Khim. Istechnikam Toka* **13** (1978) 18.
- [26] A. C. Simon and S. M. Caulder, in 'Advances in Lead-Acid Batteries' *op. cit.* [18].